The Characterization of GNA11/GNAQ Inhibitors in Uveal Melanoma Treatment

Hannah Farley

Yorktown High School

Abstract

In the cancer treatment field, a focus on targeting proliferative mechanisms in tumors has led to a lack of research in dormancy, cancer cell viability despite long disease-free periods. This is the most relevant to cancers like uveal melanoma (UM), which has a 98% recurrence rate (Seftor, 2002). To understand dormancy in UM, NR2F1 was at first determined to act as a tumor suppressor. Discovering this gene's relation to cancer growth would allow the effect of a treatment be understood by measuring the changes in NR2F1's expression level. Then, the main mutation that drives metastatic uveal melanoma, GNA11/GNAQ, was inhibited using YM-254890. The effect of this inhibition was seen by the direct correlation of an increase in NR2F1 levels in relation to the increase in the treatment YM-254890. In tumors with more than 8 cells, the more drastic increase in NR2F1 and therefore the onset of a greater dormancy phenotype is apparent.

Inducing dormancy could be the next topic of interest in cancer treatment to prevent the onset of recurrences. While this inhibition was successful in cell lines, focusing on the effectiveness of using GNA11/GNAQ inhibitions in inducing dormancy in uveal melanoma in an animal model is essential in the future.

Introduction

As cancer treatment evolves, the understanding of how cancer develops needs to as well. The current standard of care, chemotherapies, target tumor growth factors as they are what drives the cancer growth (Cancer Research UK,2017). Due to this, there is a lack of effective treatments for cancers in dormant states because they are not expressing any proliferative factors that chemotherapies can target. Dormant cancer cells can be latent for up to 15 years in some cancers after treatment, such as UM. These cells grow undetected in patients until it is discovered at stage IV where there are no viable treatment options, causing a median patient survival rate of 6-12 months after diagnosis (Francis, 2016). By studying the genetic mechanisms in uveal melanoma that allow the cancer to remain undetected in its dormant state, new treatments for cancer residual disease could be implemented.

Review of Literature

Current Treatments

While there has been major progress in understanding cancer treatment overall, therapies for residual disease have not had the same breakthroughs. Currently, most treatments are focused on the targeting of primary tumors using chemotherapies/immunotherapies, and surgery (Mayo Clinic, 2019). However, many cancers have or acquire resistance to these treatments. 90% of failures in the chemotherapy during the invasion and metastasis of cancers are related to drug resistance (Mansoori, 2017). Ultimately, surgery is the best option, but can only be used as a cure before the cancer metastasizes. In uveal melanoma, even though the success rate for local treatment is above 90%, more than half of these patients ultimately develop stage 4 uveal melanoma because cancer cells have already disseminated from the eye to the liver (Francis, 2016).

There are 3 main groups of cancer therapy (Figure 1A-C). For all of them to be successful, the aspects of cancer growth need to be understood for the full potential of these therapies to be utilized. An upregulation of dormant genes would be needed or dormancy genes need to be turned off for its proliferative genes to become active and targetable (Figure 1A & 1B). Lastly, the factors that can be specific enough to only target dormant cells must be found or the cytotoxicity could kill patients (Figure 1C).

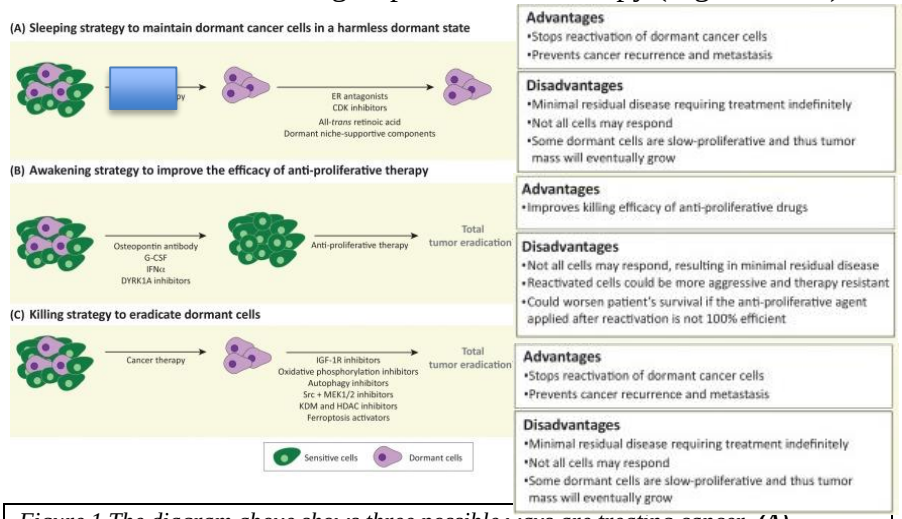

Figure 1.The diagram above shows three possible ways are treating cancer. ***(A)*** *Continuously maintain cancer in a dormant state to prohibit malignancy.* ***(B)*** *Make dormant cells become proliferative so they can be targeted by current therapies.* ***(C)*** *Target the dormant tumor cells directly. (Recasens, 2019).*

GNAQ and GNA11

In uveal melanoma two genetic mutations, nucleotide-binding proteins Q polypeptide (GNAQ) or alpha 11 (GNA11). These genes encode a G-protein alpha-subunit that mediates signals from G-protein-coupled receptors (GPCRs) to the mitogen-activated protein kinase (MAPK) pathway (Van Raamsdonk, 2009). Somatic mutations, which are usually mutually exclusive in either GNAQ or GNA11, have been revealed in a number of melanocytic neoplasms, including over 85% of uveal melanomas, making these two mutations the most

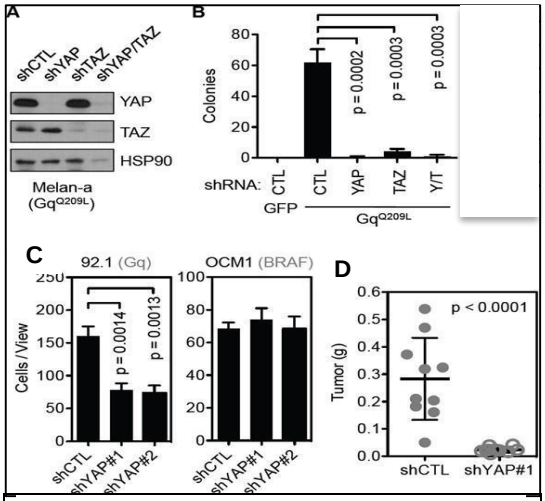

Figure 2. ***(A)*** *Western blot* ***(B)*** *Cell colonies where YAP/TAZ were more active show less cells.* ***(C)*** *cells present in YAP/ TAZ.* ***(D)*** *The tumor size /YAP (Van Raansdonk, 2009).*

prominent (Francis, 2016). This mutation has been shown to upregulate YAP (Yes-associated protein), a protein involved development and growth in the Hippo-YAP pathway (Van Raansdonk, 2009). The effect of YAP/TAZ on cancer growth is demonstrated below, where the western blot confirms the silencing of YAP/TAZ (Figure 2A). The importance of YAP/TAZ in driving cancer growth is shown by the lower number of colonies, the lower cell count, and the lower mass of the tumor by the decrease in the tumor size. (Figure 2B-D) The impact of inhibiting the mutation that regulates YAP, however; has yet to be explored as a viable therapy.

PRAME (Preferentially Expressed Antigen of Melanoma)

There are many indicators of metastasis in cancer such as PRAME is one of the factors of uveal melanoma that appears to related to its metastatic phenotype. There are two main phenotypes in cancer, dormant and metastatic. The metastatic is active when the cancer is dividing and migrating to other areas. The other form of cancer is the dormant form which is when cancer cells seem to only change into this form when there is major changes in their tumor-micro-environment. These changes can be caused by the introduction of a drug/treatment or the when cell enters a new environment, as seen by the long dormancy periods uveal melanoma has once the cells metastasize to the liver.

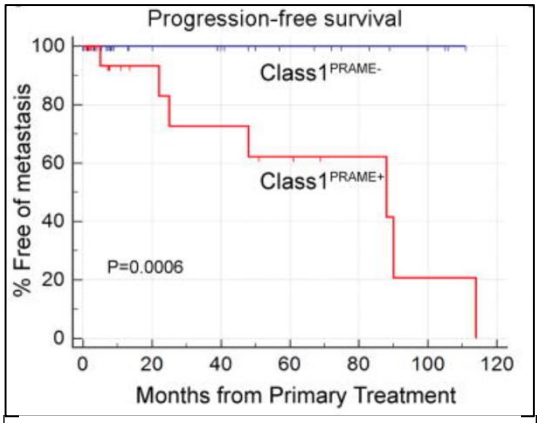

Figure 3. The graph shows the difference in between PRAME positive and negative groups in developing metastases. (Field, 2016)

PRAME appears to be an indicator of that metastatic phenotype. As shown in Figure 3, the progression-free survival of two groups, PRAME negative and positive were compared over a period of 120 months (10 years). At the time of diagnosis, both groups of class 1 (lower risk

melanoma) were free of metastasis. However, after 5 years a little less than half of the patients were metastasis free in the PRAME positive group, and by ten years all patients had developed metastases. In the PRAME negative group, none of the patients ever developed metastases, even after ten years. Through identifying factors like PRAME, precision medicine can be utilized to meet a patient's specific needs. An example to demonstrate this if pathology shows a patient's cancer to be positive for PRAME, then routine scanning for cancer metastasis will be much very more beneficial for that patient that others whose cancers are negative for PRAME and wouldn't metastasize anyway. By identifying the specific genes that cause proliferative and dormant phenotypes, the prognosis and treatment of cancer will be ameliorated.

Problems

P.$_1$: The effectiveness of silencing the GNAQ mutation on uveal melanoma growth is currently unknown.

P.$_2$: The relationship between NR2F1 and indicators of proliferation is unknown.

Objectives

Obj.$_1$: Determine how different concentrations of GNAQ inhibitor impact uveal melanoma growth.

Obj.$_2$: Determine the relationship between NR2F1, an indicator of dormancy, and PRAME and YAP, indicators of proliferation.

Hypotheses

H.$_1$: The cell lines that given the mutation inhibitor will exhibit lower levels of metastatic factors as the driver of cancer growth is silenced.

H_2: NR2F1 will have an inverse relationship with factors that drive Uveal Melanoma growth such as PRAME, and as they have opposite functions in cell growth.

Methodology

Role of Student vs. Mentor

The student participated in a lab project for a total of 16 weeks for the past two summers. During this time, the student performed siRNA preparation, qPCR, and slide preparation for immunofluorescence. The student alone was responsible for image analysis, determined the procedure, and collected data from the slide images. Student observed the mentor during image capturing using the confocal and qPCR processing using QuantStudio 3 Real-Time qPCR machine by Thermofisher. The mentor was also responsible for administering siRNA to the OMM1.3 cells before siRNA Analysis and using Graph Pad Prism 8 performed statistics.

siRNA Analysis

Lyse samples and separate phases. Before the level of gene activity can be determined, the RNA must be extracted from the cells. After the media had been removed from the cells 0.4mL of TRIzol reagent (guanidinium thiocyanate) per $1x10^5$ cells were added (in total .4mL was used). The TRIzol Reagent functioned to lyse the cells while preserving their RNA, DNA, and proteins for analysis. The solution was then pipetted up and down for homogenization. Phase separation was then conducted using 0.2mL of Chloroform per 1mL of TRIzol to separate the DNA and proteins from the RNA so pure RNA could be collected. An incubation of 2-3 minutes allowed the

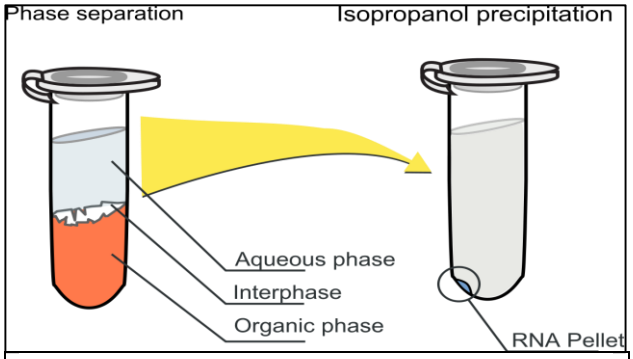

Figure 5. Diagram showing the three phases of biological components after centrifugation with chloroform. RNA is located in the aqueous layer, DNA in the interphase, and proteins in the organic phase (Farley, 2018).

chloroform reaction to occur, and then the samples were centrifuged for 15 minutes at 12,000 x rpm at 4 °C. This separates the solution into the lower pink phenol-chloroform, the interphase, and a colorless upper aqueous phase (Figure 5). The aqueous phase containing the RNA removed for analysis while the other biological components were discarded as only the RNA is needed for the RNA quantification.

Precipitate the RNA. The first step towards RNA purification is to recover the RNA from the aqueous phase that was collected. For this, 0.5mL of isopropanol per 1mL of TRIzol Reagent was added to the solution, as the salt in isopropanol neutralizes the charge on the nucleic acid backbone, causing the RNA to become less hydrophilic and precipitate out of solution for later purification. The RNA precipitate was incubated for 10 minutes before centrifugation at 12,000 x rpm at 4 °C for 15 minutes. By the end of this process, the RNA had formed a gel-like white pellet at the bottom of the tube. The supernatant was then removed through pipetting and the RNA pellet was prepared for washing.

RNA wash. The pellet was suspended in 1 mL of 75% ethanol per 1 mL of TRIzol Reagent, since ethanol can remove any salt residue from the isopropanol. The sample was then washed once and centrifuged for 5 minutes at 7500 x rpm 4 °C for RNA pellet recovery. The pellets were then left to air dry for 10 minutes. Lastly, the RNA was solubilized by resuspending the pellet in 20µl of RNAse-free water to prevent contamination.

RNA yield. Nanodrop technology was used by the mento to determine the amount of RNA per 1µl. These quantities are used to determine the amount of primers needed for DNA replication during the qPCR process. The qPCR was performed using QuantStudio 3 Real-Time qPCR machine by Thermofisher. Quantifying the DNA levels of NR2F1 after silencing on downstream targets shows the impact NR2F1 has on other genes in the pathway. Understanding

the interactions between these genes aids in mapping the specifics of cellular pathway and ultimately allows the mechanisms by which cancer grows and resistance treatsments to be understood and targeted.

Immunofluorescence

Slide hydration. The slides containing the tissue were soaked in Xylene for 5 minutes twice, as it is a clearing agent miscible with paraffin and ethanol. Then, the slides were soaked in 100% ethanol for 5 minutes twice, and then in ethanol solution decreasing by 10% until 70% solution (90%, 80%, 70%) for 3 minutes each. The decreasing concentration of ethanol (and therefore increasing concentration of water) allows the tissues to rehydrate slowly which prevents possible damage to the cells from cytolysis. After the ethanol, the tissues are immersed in water twice for 3 minutes.

Heated antigen retrieval. The slides were placed in 500mL of 10 mM citrate buffer at pH 6.0. The citrate buffer breaks cross-links between antigens, and unmasks them as shown in (Figure 6). The slides were heated under pressure for 15 minutes at high pressure. The slides were then submerged in water and phosphate buffer saline (PBS) to remove the citrate buffer before and return pH levels to from acidic to neutral.

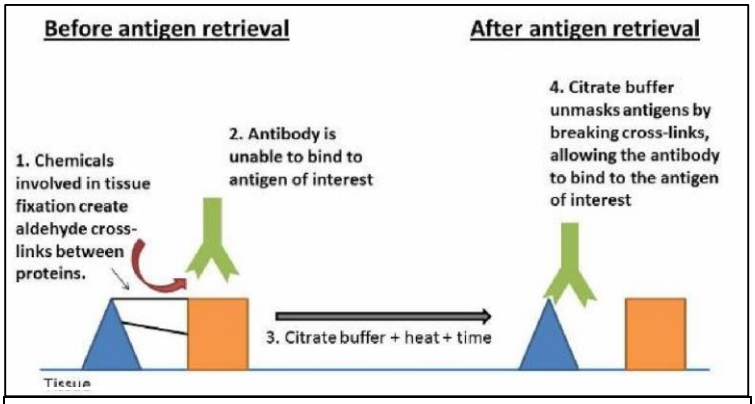

Figure 6. The antigen revival process needed for the fluorescence staining (Leinco,2002).

Permeabilization and blocking. Permeabilization provides access to the inside of the cell as it dissolves lipids from the cell membrane to make them permeable to antibodies. This is necessary for the staining of DAPI and other targets that are found within the cytoplasm and nucleus, as they would not be able to enter the cell otherwise. Therefore 1% Triton X-100 in PBS was administered to the tissue on the slides for 5 minutes to begin the permeabilization process as Triton X-100 permeabilizes cellular membranes (Figure 7). Triton was used specifically because the target gene NR2F1 is localized in the nucleus. The PBS was then utilized again for cleaning purposes. The samples were then blocked with 50mM ammonium chloride (NH4Cl) for 30 minutes and blocking buffer (0.3g bovine serum albumin in 10mL PBS + 150µl of Normal Goat Serum) for 60 minutes. This helped prevent non-specific antibody bonding by covering free sites on the membrane. The primary antibody was administered overnight, and then the tissues were washed 3 times with PBS +0.02% Tween for 10 minutes at room temperature. The tween serves to prevent non-specific binding as well as remove excess antibodies. The blocking buffer was then applied again for 60 minutes to prepare for the fluorophores. The fluorophores MelanA (Goat anti-mouse AF546-Red) and NR2F1 (Gist anti-rabbit 488-green) were both prepared in 1:200µL ratio to the blocking buffer. The fluorophores were administered to the tissue and were incubated 1 hour at room temperature. After another 3

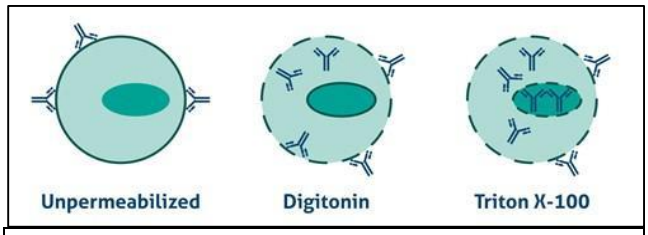

Figure 7. Diagram of antibodies binding to an unpermeabilized cell, one treated with Digitonin and one treated with TritonX-100. Triton X-100 is the only one where the antibodies could penetrate the nucleus (Proteintech,2017).

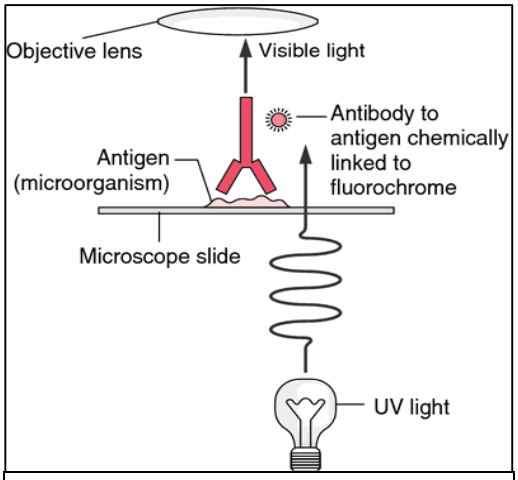

Figure 8. Diagram depicts how the confocal microscope analyzes slides (University of Queenlands, 2019).

washes with PBS + 0.02% Tween, the slides were incubated with Hoechst stain solution for 30 minutes to stain the nuclei of the cells. Hoechst was used instead of DAPI because it can pass through cell membranes without permeabilization. Before mounting the tissue, a final 3 washes with PBS + 0.02% Tween, 10 minutes each were done to remove the Hoechst. The slide preparation concluded with mounting of the slide cover with Prolong anti-fade without DAPI. The slides were kept in the dark overnight to prevent the fluorophores from fading. The slides were then analyzed using a confocal microscope and regions of interest were captured (Figure 8).

Picture Analysis

ImageJ. Before analysis, OMM1.3 cells were given different concentrations of YM-254890 inhibitors (0μL, 100μL, 200μL, and 300μL) as it inhibits Gα11/Gαq mutations, the main oncogenes driving uveal melanoma growth. Each concentration was balanced with Dimethyl Sulfoxide (DMSO) so every group received a total of 300μL of treatment over a period over 14 days. The resulting levels of NR2F1, MelanA, and Caspase were measured using ImageJ software by Java. First, a mask for individual cell measurement was created. This would allow for individual cells or tumors to have their fluorescence (the quantity of the target gene expressed) measured. This was done by adjusting the threshold of the image, and then selecting "create mask". The final step was to "analyze particles", where a minimum object size of 30μm and an eccentricity between 0.5 and 1 were determined to be the proper parameters for cell measurement to exclude cellular debris.

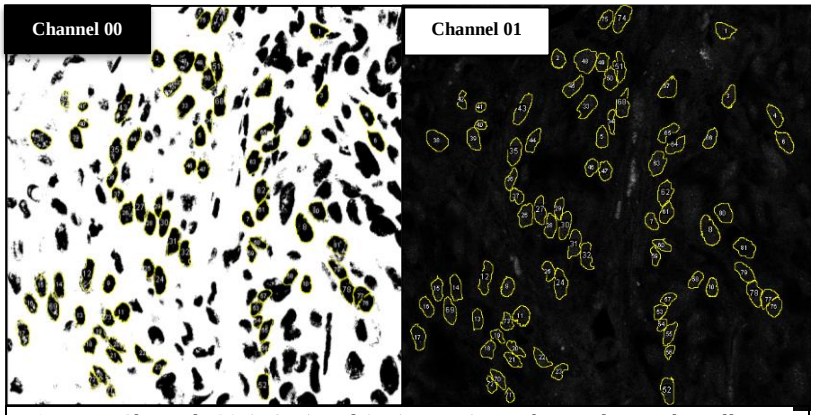

Figure 9. Channels 00 (DAPI) and 01 (NR2F1) are shown above. The cell outlines created on DAPI act as a mask to measure the expression of the fluorescence of specific cells in other channels (Farley, 2019).

The cell outlines were then transferred onto another channel for measurement where the cell outlines from the DAPI (channel 00) were transferred onto the NR2F1 (channel 01) to measure NR2F1 intensity on those specific cells (Figure 9). The last channel (channel 02) was a specific staining of a factor (PRAME, MelanA, or Caspase 3) whose relationship with NR2F1 could be determined by comparing the levels of fluorescence of both factors in a single cell.

Statistical analysis. All statistical analysis was done using an unpaired t-test with a Gaussian distribution in the Graph Pad Prism 8 program. A t-test was used as we would expect the mean of the control population that was given no drug to differ significantly from the mean of the experimental population which was given the YM-254890 inhibitor.

Results

Phase 1

Silencing of NR2F1. There was a change in the expression of target genes when NR2F1 was manipulated. The level of NR2F1 expression was altered using small interfering RNAs (siRNA). To ensure that the silencing worked properly, the level of NR2F1 produced over 24 hours, 48 hours, 72 hours and 96 hours was measured, allowing us to see the decrease in NR2F1 expression while the siRNA is still active and the increase in expression by the time it wears off (Figure 10). The is because the silencing of genes using

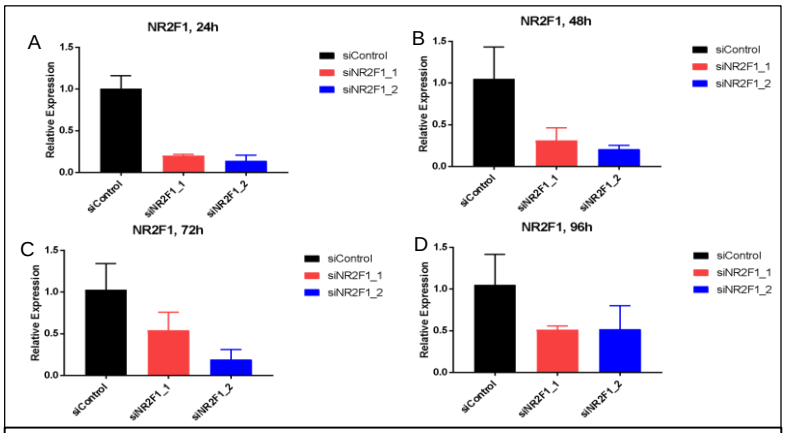

Figure 10. ***(A)****NR2F1 relative expression 24 hours after siRNA exposure.* ***(B)*** *NR2F1 relative expression 48 hours after siRNA exposure.* ***(C)*** *NR2F1 relative expression 72 hours after siRNA exposure.* ***(D)*** *NR2F1 relative expression 96 hours after siRNA exposure.*

siRNA is only effective in suppressing gene levels for approximately 24 to 48 hours, so the decrease and then gradual increase in gene expression is expected.

Since the expression of NR2F1 affects the tested genes through a downstream method, and therefore there is no direct relationship between NR2F1 and other gene ‘s expression. Due to this, the overall gene activity will need to be examined over more than one day as any changes in NR2F1 expression will not immediately affect the other gene. This can be accomplished by studying gene expression over 2 days, and determining changes in gene expression every 24 hours. At 24 hours, both of the silenced groups showed lower quantities of gene expression than the control, and at 48 hours the NR2F1 expression had started to return to normal after the treatment, which demonstrates how siRNA only lasts about 24-48 hours (Figure 10A, 10B). This is further demonstrated after 96 hours both siNR2F1’s began to increase in expression level again (Figure 10D).

Growth Factor CTGF. Connective Tissue Growth Factor (CTGF) has been documented to be involved in cell migration, invasion, and in some cases cell proliferation. It was previously reported to be expressed 35 times higher in metastatic vs. non-metastatic UM when comparing microarray data (Seftor, 2002). Based on these results, it was decided to test if this gene would be affected when NR2F1 was silenced. At 24 hours the levels of the gene are low, with the si-1 and si-2 levels barely differentiating from the siControl (Figure 11A). As time progress to 48 hours, gene levels begin

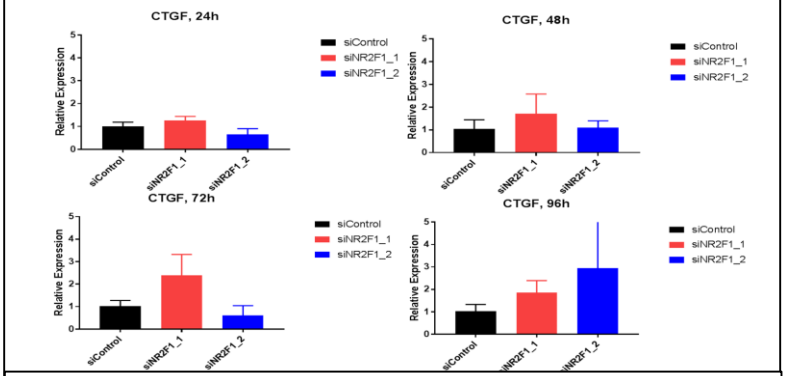

*Figure 11. (**A**) CTGF relative expression 24 hours after NR2F1 silencing. (**B**) CTGF relative expression 48 hours after NR2F1 silencing. (**C**) CTGF relative expression 72 hours after NR2F1 silencing. (**D**) CTGF relative expression 96 hours after NR2F1 silencing.*

to rise rapidly for the si-1 group while the si-2 group began a slow growth upward. At 72 hours, si-1 reaches almost three times its relative expression while si-2 is at its normal relative expression (Figure 11B, 11C). At the end of the measuring period si-2 relative expression for CTGF drops to twice its normal expression levels while si-2 increases to about 3 times relative expression (Figure 8D). The increase in CTGF levels overtime in correspondence to NR2F1's downregulation suggests an indirect relationship between the genes. When comparing this inverse in expression to the function of the genes themselves, it can be determined that CTGF does have a proliferative function in uveal melanoma.

Growth Factor CYR61. Cytosine-rich angiogenic inducer 61 (CYR61) is an extracellular protein that is involved angiogenesis, inflammation, and matrix remodeling. Based on these functions, it was hypothesized that CYR61 would be upregulated in UM. At 24 hours levels of both si-1 and si-2 haven't been modified greatly from normal expression (Figure 12A). By 48 hours, si-1 increased dramatically while si-2 levels expressed very little change (Figure 12B). This is concurrent with the change in CTGF, levels, and may have been the results in the difference of the types of siRNA used. Levels at 72 hours demonstrate that si-1 has reached approximately 3.5 times normal relative expression, while si-2 continues to be at expression by remaining at 100% expression (Figure 12C). In 96 hours si-1 had tripled levels of normal expression while si-2 had doubled levels of relative

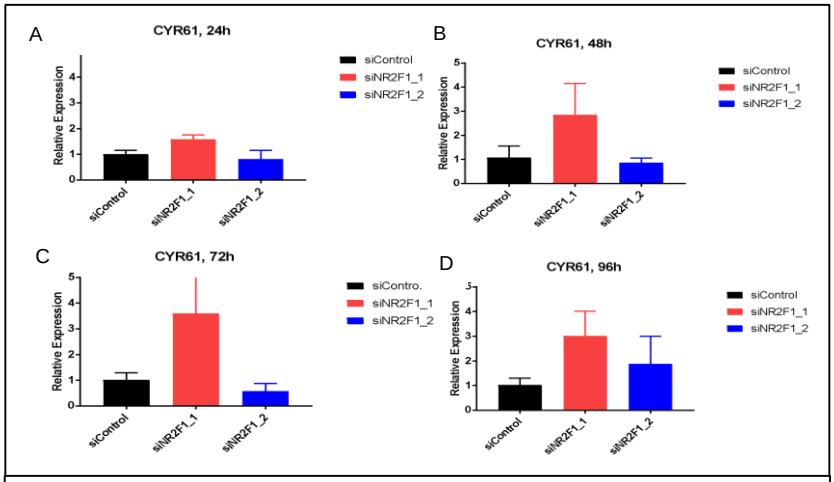

*Figure 12. (**A**) CYR61 relative expression 24 hours after NR2F1 silencing. (**B**) CYR61relative expression measured 48 hours after NR2F1 silencing. (**C**) CYR61 relative expression 72 hours after NR2F1 silencing. (**D**) CYR61 relative expression 96 hours after NR2F1 silencing.*

expression (Figure 12D). CYR61 showed a positive change in expression over the 4 days after NR2F1 silencing, justifying its role in UM proliferation.

Growth Factor ANKRD1. Ankyrin Repeat Domain 1 (ANKRD1) is a transcription factor involved in cell growth and response to stress. Based on this function, this gene was tested to see if there was a change in the level of expression when NR2F1 was silenced. At 24 hours the ANKRD1 levels for both si-1 and si-2 were above the levels of the siControl, with si-2 about double the normal relative expression and at 48 hours both groups showcase the relative expression of about four times normal expression (Figure 13A, 13B). At 72 hours this expression decreases slightly due to possible changes in the suppression of NR2F1, but recovers by hour 96 (Figure 13C). The rapid rise in ANKRD1 levels after dormancy gene NR2F1 silencing demonstrate its role in UM proliferation.

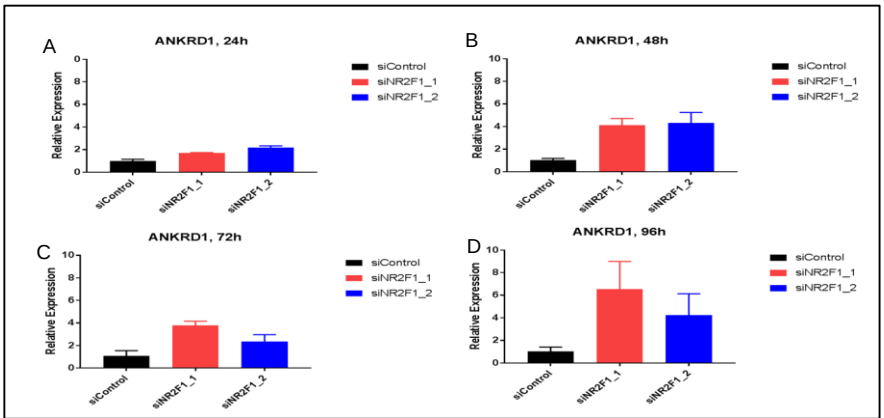

*Figure 13. (**A**) ANKRD1 relative expression 24 hours after NR2F1 silencing. (**B**) ANKRD1relative expression measured 48 hours after NR2F1 silencing. (**C**) ANKRD1 relative expression 72 hours after NR2F1 silencing. (**D**) ANKRD1relative expression 96 hours after NR2F1 silencing.*

(Space intentionally left blank)

Phase 2

NR2F1 Expression in Different Cell Types. It was previously confirmed that NR2F1 was an important gene in regulating division in uveal melanoma, and thus had a role in the

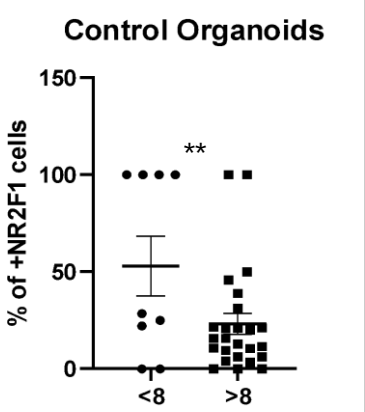

Figure 14. Percentage of NR2F1 in UM cancer metastatic clusters small (<8 cells) and large (>8 cells) (Figure by H. Farley).

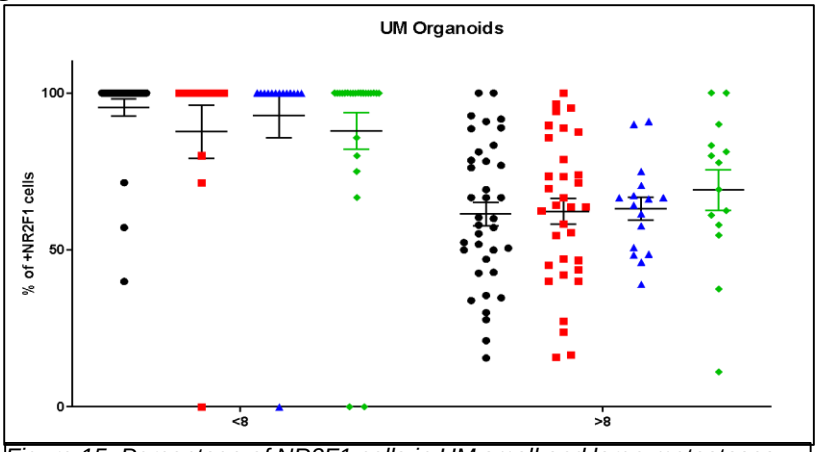

Figure 15. Percentage of NR2F1 cells in UM small and large metastases. Black represents the control, red 100um of drug, blue 200 um of drug, and green 300um of drug (Figure by H. Farley)

cancer's dormancy mechanisms. It remained to be seen if NR2F1expression would differ between UM cells at differ growth rates, with large tumors in a metastatic state growing faster than dormant single cells. When comparing these two types of cells, NR2F1 levels were demonstrated to be much lower in cell clusters with more than 8 cells in UM cells that received no treatment (Figure 14). The cells that were treated with the YM inhibitor showed similar results when there were less than 8 cells present, with a vast majority of the cells groups being at least 50% positive for NR2F1 (Positivity was determined by the number of determined NR2F1 cells/the total number of cells). Eight cells was chosen as a parameter for small and large metastases as it is a potential middle ground between small and large groups. There was no significant difference between the percent of positive NR2F1 between YM concentrations in the cell after 14 days of treatment (Figure 15). This may have been because the cultured cells may have been too confluent (too close together) and therefore were not growing properly. To counter

this the cells were given a longer time to grow (30 days). The percentage of positive NR2F1 in the second control is demonstrated to be even more statistically significant ($p<.001$) for the percentage of NR2F1 in the cells compared to the first control organoid (Figure 14 & 16).

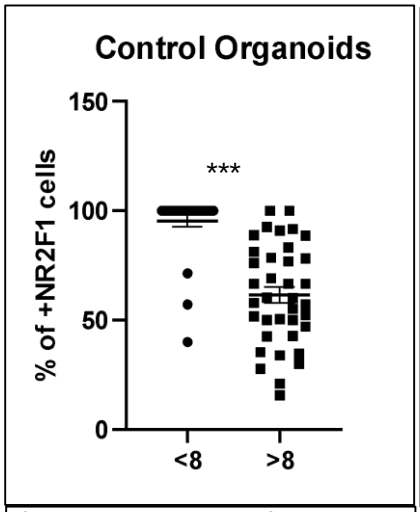

Figure 16. Percentage of NR2F1 positive cells across different concentrations of YM inhibitor.

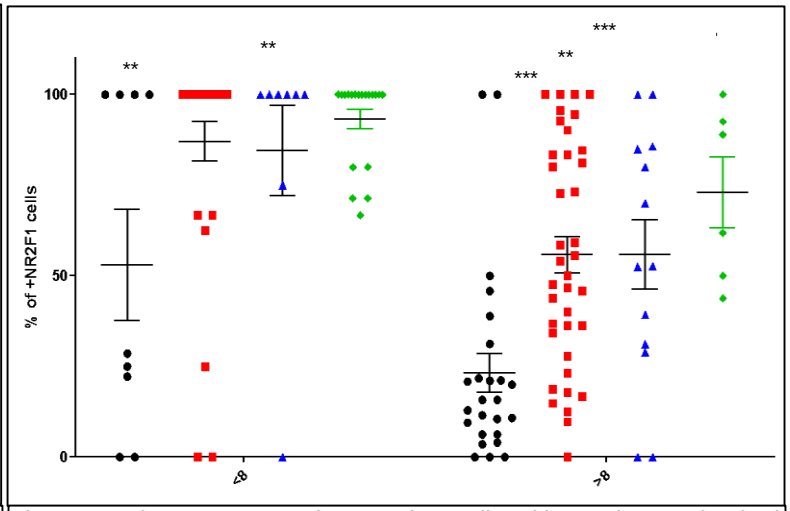

Figure 17. The percentage of NR2F1 in small and large clusters that had been treated with the YM at different concentrations. Black is the control, red is the drug at 100um, blue at 200um, and green at 300um.

A clear significance can also be seen between the control group and the cells that were treated with 300um of YM-inhibitor, as the treated cells expressed much higher levels of NR2F1.

Discussion

In the phase one of this experiment, NR2F1 was determined to be involved in uveal melanoma (UM) dormancy mechanisms demonstrated by the increase in growth factor expression following the silencing of NR2F1. However, there was no obvious relationship between NR2F1 and the tumor suppressors. We expected the expression of tumor suppressor genes to decrease after NR2F1 silencing as both are involved dormancy, but there was little decrease in expression over 96 hours. This study was limited by the fact that gene expression was only examined between 24-96 hours after silencing of NR2F1, so any changes in expression before or after this time were unable to be seen. The goal of this phase was to determine NR2F1's role in quiescence, and its relationship with the tumor growth factors supports this despite the lack of relationship between NR2F1 and tumor suppression factor expression.

a)

The establishment of NR2F1 as a dormancy indicator was used to determine the effect of GNA11/GNAQ inhibitors in uveal melanoma treatment. As previously established, Gaq mutations make up 85% of metastatic uveal melanoma, and the inhibition of this mutation has been explored through the use of the inhibitor YM-256890. However, the impact of this inhibitor on cancer has yet to be seen in respect to inducing dormancy. Big changes in the tumor micro-environment, such as the introduction of a treatment, induces dormancy as the cancer tries to preserve itself from the proliferative-targeted therapy. If this happens, then the chance of residual disease from the treatment is higher because the dormant cancer was unaffected by a proliferative-oriented treatment. Therefore, the expression of NR2F1 in a tumor after treatment with YM-inhibitor was examined to see the impact the drug has on the cancer phenotype. In the control group that was not treated with the YM inhibitor, NR2F1 was shown at a higher quantity in cell clusters less than eight. This is most likely due to the fact that cells in clusters larger than 8 are metastatic tumors, while smaller clusters are dormant cells that had barely begun to divide. In cell clusters greater than 8 it is demonstrated that the control group had low levels of NR2F1 as a large proliferating tumor would not express high levels of a dormancy gene. The difference in the number of these cells likely affects the tumor micro-environment and the phenotype of these cells. The importance of the GNA/GNA11 mutation in driving UM growth is demonstrated by the increase in dormancy gene NR2F1 expression after the mutation's inhibition using YM-256890. This means that the cells acquired a dormant phenotype upon the inhibition of the GNAQ/GNA11 pathway. It is also demonstrated that as the concentration of the YM inhibitor increased, the percentage of cells that were positive for NR2F1 increased as well, and the total number of cell colonies decreased. This indicates that not only does the YM inhibitor force some cancer cells into dormancy but it also appears to destroy cells in the metastatic phase.

Applications

NR2F1's relationship with these specific genes has never been tested before in UM and through this study have now been established as inducers of metastasis in this type of cancer. Understanding these relationships between genes is crucial for treatment design and application. Without understanding NR2F1's role in dormancy, the impact of Gaq inhibition on UM cancer growth could have never been realized. YM-inhibitors appear to destroy cancer cells in the metastatic state and induce a state of dormancy in the residual cells, which serve to function as the treatment of residual disease (Figure 1A). Currently, there are no effective treatments for metastatic uveal melanoma (UM), therefore keeping the cancer in a dormant state through the use of YM-inhibitors would positively impact the overall survival rate.

Future Research

In the future, the relationship between NR2F1 and PRAME should be further analysed as possible indicators of cancer growth and dormancy respectively. NR2F1 has already been utilized in this study as an indicator of how the YM inhibitor affected the cancer cells, as the dormancy (NR2F1 gene expression), increased as the concentration of the YM inhibitor increased. PRAME has already been found in a variety of cancers, such as breast, lung, and other melanomas besides UM (Field, 2019). The changes in PRAME expression can be utilized to determine the effect of a treatment just like NR2F1 was in our study on cancer growth. The inhibition of the GNA11/GNAQ pathway has been studied in a clinical setting, but there has been a failure to see the same dormancy effect on the cancer in the patient model (Croce, 2019). Our understanding with NR2F1's dormancy relationship to the pathway will be helpful in determining why there is a difference between the cell line and patient models.

Conclusion

The objective of this study was to determine NR2F1's role in the dormancy mechanism of UM and to then determine the effect of YM inhibitors on uveal melanoma growth using NR2F1 as an indicator of dormancy. To accomplish this NR2F1 was silenced by siRNA and measured over a period of 24 intervals. The hypothesis of NR2F1 being involved in UM dormancy is supported by our data. Most of the genes that were showed an increased expression after NR2F1 was silenced. However, not all of the genes had such a clear expression pattern, showing that NR2F1's relationship with its downstream factors is more complex than previously believed. Different concentration of the YM inhibitor were administered to cells to determine the effect of YM inhibitors on uveal melanoma and they were allowed to grow over 30 days after a week of YM treatment. The hypothesis of YM-inhibition reducing cell growth was supported by the increase in the dormancy phenotype. The percentage of positive NR2F1 was then determined using a specific parameter and to separate positive cells from the background and precipitate. There was a positive correlation between the YM concentrations and the percentage of NR2F1 positive cells seen, meaning that the YM inhibitors were effective in turning off the GNAQ/GNA11 mutation that was driving the cancer growth and allowed the cells to convert back into a dormant state.

Works Cited

CALIPHO Team - SIB - Swiss Institute of Bioinformatics. (2019, January 11). CYR61 - Function. Retrieved July 30, 2019

Cancer Research UK. (2017, November 15). General cancer information. Retrieved October 8, 2019,

Francis, J., Halpern A. (2016, September/October). Skin Cancer Foundation. Retrieved July 30, 2019,

Field, M. G., Decatur, C. L., Kurtenbach, S., Gezgin, G., van der Velden, P. A., Jager, M. J., … Harbour, J. W. (2016). PRAME as an Independent Biomarker for Metastasis in Uveal Melanoma. *Clinical cancer research : an official journal of the American Association for Cancer Research*, *22*(5), 1234–1242. doi:10.1158/1078-0432.CCR-15-2071

Leinco. (2002). Immunohistochemistry. Retrieved October 3, 2019,

Mansoori, B., Mohammadi, A., Davudian, S., Shirjang, S., & Baradaran, B. (2017). The Different Mechanisms of Cancer Drug Resistance: A Brief Review. *Advanced pharmaceutical bulletin*, *7*(3), 339–348. doi:10.15171/apb.2017.041

Mayo Clinic. (2019, April 5). Cancer treatment. Retrieved October 9, 2019,.

Proteintech. (2017, March 22). 9 Tips to optimize your IF experiments. Retrieved August 14, 2019,

University of Queensland. (2019, August 22). Confocal Microscopes. Retrieved October 3, 2019

Valpione S, Moser JC, Parrozzani R, et al. Development and external validation of a prognostic nomogram for metastatic uveal melanoma. *PLoS ONE* 2015; 10(3):e0120181. doi:10.1371/journal.pone.0120181.

Van Raamsdonk CD, Bezrookove V, Green G, et al. Frequent somatic mutations of GNAQ in uveal melanoma and blue naevi. *Nature* 2009; 457(7229):599–602. doi:10.1038/nature07586.

Yu, F. X., Luo, J., Mo, J. S., Liu, G., Kim, Y. C., Meng, Z., … Guan, K. L. (2014). Mutant Gq/11 promote uveal melanoma tumorigenesis by activating YAP. *Cancer cell*, *25*(6), 822–830. doi:10.1016/j.ccr.2014.04.017